5. Tanaka E, Kimoto T, Tsuyuguchi K, et al. Effect of clarithromycin regimen for Mycobacterium avium complex pulmonary disease. Am J Respir Crit Care Med 1999;160:866–72.
6. Field SK, Cowie RL. Treatment of Mycobacterium avium-intracellulare complex lung disease with a macrolide, ethambutol, and clofazimine. Chest 2003;124:1482–6.
7. Kobashi Y, Matsushima T. The effect of combined therapy according to the guidelines for the treatment of Mycobacterium avium complex pulmonary disease. Intern Med 2003; 42:670–5.
8. Griffith DE, Brown BA, Cegielski P, et al. Early results (at 6 months) with intermittent clarithromycin-including regimens for lung disease due to Mycobacterium avium complex. Clin Infect Dis 2000;30:288–92.
9. Ono N, Satoh K, Yokomise H, et al. Surgical management of Mycobacterium avium complex disease. Thorac Cardiovasc Surg 1997;45:311–3.
10. Shiraishi Y, Nakajima Y, Takasuna K, et al. Surgery for Mycobacterium avium complex lung disease in the clarithromycin era. Eur J Cardiothorac Surg 2002;21:314–8.
11. Pomerantz M, Madsen L, Goble M, et al. Surgical management of resistant mycobacterial tuberculosis and other mycobacterial pulmonary infections. Ann Thorac Surg 1991;52: 1108–11.
12. Tsunezuka Y, Sato H, Hiranuma C. Surgical outcome of mycobacterium other than mycobacterium tuberculosis pulmonary disease. Thorac Cardiovasc Surg 2000;48:290–3.
13. Nelson KG, Griffith DE, Brown BA, et al. Results of operation in Mycobacterium avium-intracellulare lung disease. Ann Thorac Surg 1998;66:325–30.
14. Kobashi K, Matsusima T. Comparison of clinical features in patients with pulmonary Mycobacterium-avium complex (MAC) disease treated before and after proposal for guidelines. J Infect Chemother 2004;10:25–30.

日外会誌　107（6）：262～267，2006

特　集

# 縦隔疾患に対する外科的アプローチ

## 3. 胸腺上皮性腫瘍の外科治療成績

慶應義塾大学医学部外科

堀之内宏久，朝倉　啓介，木村　吉成，竹内　　健
川村　雅文，渡辺　真純，江口　圭介，小林　紘一

キーワード　胸腺腫，胸腺癌，正岡分類，WHO 分類，外科治療

### I. 内容要旨

胸腺腫を含む胸腺上皮性腫瘍は頻度の多い腫瘍ではない．大半の胸腺種は外科治療によって良好な予後が得られるものの，術後の再発，進展を呈する症例では治療に難渋することもある．当科にて1985年より2005年までの胸腺関連腫瘍のうち組織学的に胸腺腫あるいは胸腺癌と診断された症例で，予後を追跡でき，病理標本をWHO分類に当てはめて再検討した131例を対象として外科治療成績を検討した．男性76例，女性55例，平均年齢53歳（20歳から80歳）正岡の分類ではI期42例，II期43例，III期23例，IVa期15例，IVb期1例，胸腺癌（扁平上皮癌）7例であった．WHO分類ではType A 7例，Type AB 23例，Type B1 30例，Type B2 27例，Type B3 29例，Type C 15例であった．実施手術は生検5例，腫瘍切除5例，胸腺摘出5例，拡大胸腺全摘術が65例，腫瘍切除に合併切除を行った症例が4例，拡大胸腺全摘術に合併切除を行った症例が51例であった．合併切除の内訳は播種巣1例，胸膜合併切除14例，心膜合併切除が10例，肺合併切除が4例，2種類以上の組織，器官，臓器を合併切除した症例が22例であった．Masaokaの分類を用いて予後を検討したところ，5年，10年，15年生存率は，I期で100%，100%，100%，II期で100%，100%，87.5%，III期で100%，87.5%，87.5%，IVa期で71.1%，53.3%，53.3%，胸腺癌症例では42.9%，42.9%，0%であった．IVa期および胸腺癌の予後は他の病期と比較して有意に予後が不良であったが，I期，II期，III期の間には生存には有意差を認めなかった．WHO分類では，Type Aでは5年生存率100%，Type ABでは5年，10年，15年生存率が100%，100%，100%，Type B1では100%，100%，75.0%，Type B2では92.6%，86.4%，86.4%，Type B3では95.5%，95.5%，81.8%Type Cでは57.1%，42.9%，0%であった．Type Cの予後はType B3と比較すると予後の悪い傾向が認められた．Type Cとその他の群との比較ではType Cの予後が有意に不良であった．胸腺上皮系腫瘍の外科治療成績は胸腺癌も含め，病理組織学的性格と腫瘍の浸潤の程度によって決定されると考えられた．胸腺上皮系腫瘍の内でも浸潤型胸腺腫（Type B3）および胸腺癌（Type C）の治療成績は良好とは言えず，生検による病理組織学的検討と画像診断による浸潤傾向の診断を行って集学的治療を行うことが不可欠であると考えられた．

### II. はじめに

胸腺腫を含む胸腺上皮性腫瘍は頻度の多い腫瘍ではないが，進展形式と合併疾患の多様性など特徴的な性格を有する．大半の胸腺種は外科治療によって良好な予後が得られるものの，浸潤傾向が強かったり，縦隔外への進展を呈する症例では手術後遠隔期に再発を起こし，治療に難渋する症例もある．胸腺腫の外科治療成績を評価する際に基準となる評価方法は1940年代

PROGNOSIS OF SURGICALLY TREATED THYMIC EPITHELIAL TUMORS

Hirohisa Horinouchi, Keisuke Asakura, Yoshishige Kimura, Ken Takeuchi, Masafumi Kawamura, Masazumi Watanabe, Keisuke Eguchi and Koichi Kobayashi

Department of Surgery, Keio University School of Medicine, Tokyo, Japan

表1 胸腺腫症例の分布 Characteristics of assessable patients

| | No of patients | Age | Gender (M : F) | P | Myasthenia Gravis (+ : −) | P | Median follow up (Month) |
|---|---|---|---|---|---|---|---|
| Masaoka | | | | | | | |
| I | 42 | 54 (22-76) | 27 : 15 | P = 0.62 | 8 : 34 | p = 0.06 | 81 (30-232) |
| II | 43 | 52 (22-75) | 23 : 21 | | 20 : 24 | | 85 (10-195) |
| III | 23 | 53 (21-80) | 17 : 11 | | 8 : 20 | | 57 (6-202) |
| IVa | 15 | 54 (40-76) | 8 : 8 | | 6 : 10 | | 48 (0-177) |
| IVb | 1 | 66 | 1 : 0 | | 0 : 1 | | 1 |
| Ca | 7 | 62 (52-76) | 6 : 1 | | 1 : 6 | | 57 (34-177) |
| WHO | | | | | | | |
| A | 7 | 54 (49-68) | 5 : 2 | P = 0.21 | 0 : 7 | p = 0.02 | 59 (2-90) |
| AB | 23 | 48 (25-72) | 13 : 10 | | 6 : 17 | | 62 (14-232) |
| B1 | 30 | 53 (22-76) | 15 : 15 | | 10 : 20 | | 93 (6-219) |
| B2 | 27 | 52 (21-80) | 18 : 9 | | 12 : 15 | | 99 (3-207) |
| B3 | 29 | 52 (40-75) | 13 : 16 | | 14 : 15 | | 86 (12-177) |
| C | 15 | 61 (30-78) | 12 : 3 | | 1 : 14 | | 54 (0-118) |

より模索されてきた．現在まで予後を決定する因子として，正岡の分類[1]，WHO分類[2)3)]，TNM分類[4]，Grupped' Etude des Tumeurs Thymiques system[5]などが発表され，実際に臨床で用いられているが，最も予後を反映するものは正岡の分類とWHO分類であると考えられている．

正岡の分類は手術所見および組織学的な浸潤の有無による分類であり，組織学的な悪性度評価との関係が明らかでないことと，術前での評価が困難であることが欠点として挙げられていた．1985年にMarinoとMullar-Hemerinkにより胸腺腫を組織学的に分類することにより予後と相関するとの報告があり[6]，その後胸腺腫を組織学的特徴によって6つの組織型に分類するWHO分類が1999年に発表されることとなった[3]．以後，WHO分類が胸腺腫の臨床像を反映するかについて検討され，予後との相関のみならず，術前治療の指標となるとの報告がなされている[7)~9)]．今回当科で経験した胸腺腫と胸腺癌を含む胸腺上皮性腫瘍症例の外科治療成績を検討するにあたり，Retrospectiveに病理の評価を行い，臨床情報とともに検討した．

## III. 対　象

当科にて1985年より2005年までの胸腺関連腫瘍のうち組織学的に胸腺腫あるいは胸腺癌と診断された症例で，予後を追跡でき，病理標本をWHO分類に当てはめて再検討した131例を対象とした．

男性76例，女性55例，平均年齢53歳（20歳から80歳）正岡の分類ではI期42例，II期43例，III期23例，IVa期15例，IVb期1例，胸腺癌（扁平上皮癌）7例であった．WHO分類ではType A 7例，Type AB 23例，Type B1 30例，Type B2 27例，Type B3 29例，Type C 15例であった．

実施した手術は生検のみ5例，腫瘍切除5例，胸腺摘出5例，拡大胸腺全摘術が65例，腫瘍切除に合併切除を行った症例が4例，拡大胸腺全摘術に合併切除を行った症例が51例であった．合併切除の内訳は播種巣1例，胸膜合併切除14例，心膜合併切除が10例，肺合併切除が4例，2種類以上の組織，器官，臓器を合併切除した症例が22例であった．

重症筋無力症の有無では重症筋無力症の合併を認めた症例が43例，合併のない症例が88例であった．

予後をKaplan-Meier法によって生存曲線を作成し，Log rank法にて群間の有意差を検討した．各群における独立性の検定にはχ二乗検定を用いた．p≦0.05で有意差ありと判定した．

## IV. 結　果

群別に独立性を検定したところ，正岡の分類では，年齢，性別，MGの有無の項目は独立した事象であった．WHO分類では年齢，性別は独立事象と考えられたが，Type AではMG症例を認めず，WHO分類による組織型とMGの間に相関がある結果となったが，Type Aを除いて検討すると有意差はなく，MGと組織型は独立事象であった．

Masaokaの分類を用いて予後を検討したところ，5

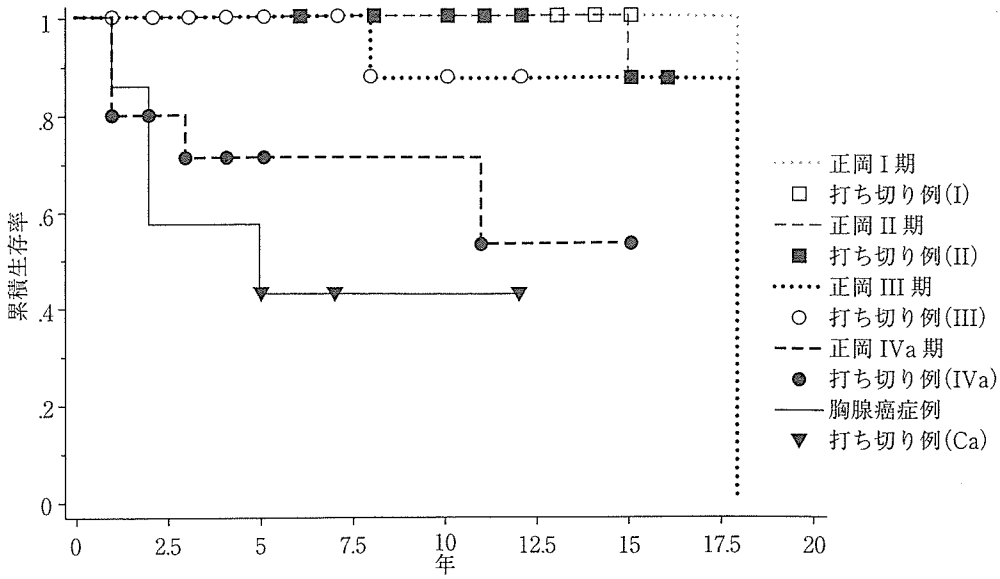


図 1　正岡分類による予後（含胸腺癌）Kaplan-Meier 法

5, 10, 15year survival in each group are 100%, 100%, 100% in Stage I, 100%, 100%, 87.5% in Stage II, 100%, 87.5%, 87.5% in Stage III, 71.1%, 53.3%, 53.3% in Stage IVa, 42.9%, 42.9%, 0% in Thymic cancer respectively. Survival of IVa and thymic carcinoma are significantly poor compare to Stage I, II, and III.

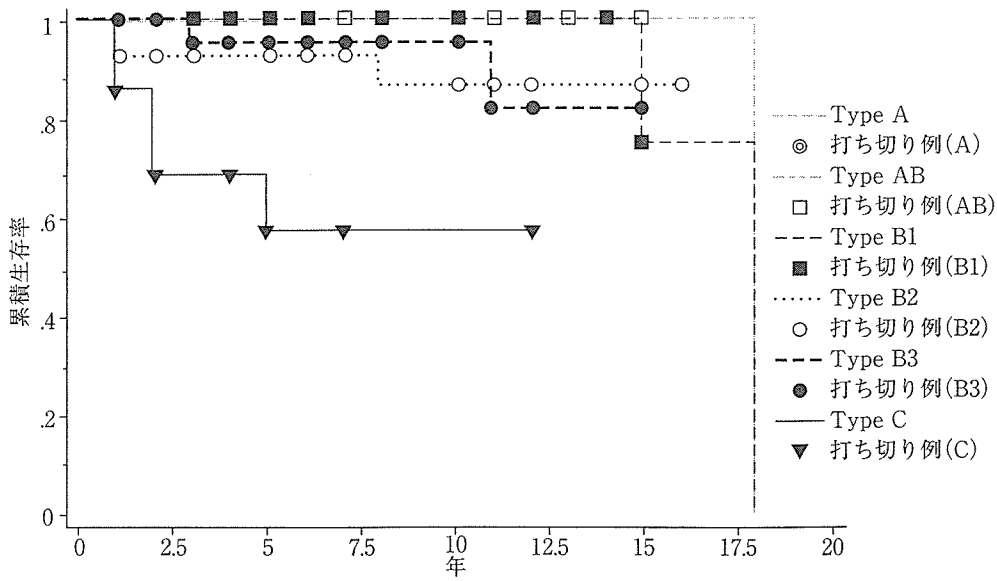


図 2　WHO 分類による予後 Kaplan-Meier 法

According to WHO classification, 5 year survival of type A was 100%, 5, 10, 15 year survival are 100%, 100%, 100%in type AB, 100%, 100%, 75.0% in type B1, 92.6%, 86.4%, 86.4% in type B2, 95.5%, 95.5%, 81.8% in type B3, 57.1%, 42.9%, 0% in type C. Survival of Type C was the poorest among all and significant difference between al other groups were recognized.

年，10 年，15 年生存率は，I 期で 100%，100%，100%，II 期で 100%，100%，87.5%，III 期で 100%，87.5%，87.5%，IVa 期で 71.1%，53.3%，53.3%，胸腺癌症例では 42.9%，42.9%，0% であった（図 1）．IVa 期お

よび胸腺癌の予後は他の病期と比較して有意に予後が不良であったが，I期，II期，III期の間には生存には有意差を認めなかった（図1）．

WHO分類を用いて予後を検討したところ，Type Aでは5年生存率100%，Type ABでは5年，10年，15年生存率が100%，100%，100%，Type B1では100%，100%，75.0%，Type B2では92.6%，86.4%，86.4%，Type B3では95.5%，95.5%，81.8%Type Cでは57.1%，42.9%，0%であった（図2）．Type Cの予後はType B3と比較すると$p=0.053$で予後の悪い傾向が認められた．Type Cとその他の群との比較では各群間と比較してType Cの予後が有意に不良であった（図2）．

## V. 考　察

胸腺上皮系腫瘍（胸腺腫および胸腺癌）の臨床的悪性度（再発と予後）については組織学的所見と乖離があることが述べられていた[5)10)11)]．1984年に発表された正岡の分類は手術所見（浸潤の程度）によって悪性度を判断する分類[1)]であるが，予後と無再発生存を良く反映するので現在でもひろく使用されている[1)12)]．しかし，正岡の分類は基本的に手術所見による浸潤傾向を臨床的に判断するもので，術前に悪性度を評価することが困難であった．

胸腺上皮腫瘍の組織学的分類はBernatzらのリンパ球の混在度と上皮性分の細胞形態から判断する分類が1961年に発表され[13)]，これに準じる分類が採用されることが多かったが，予後との関連に乏しいといわれていた[11)]．Nomoriらは核面積による予後の解析を行い[14)]，予後との関連を報告したが，臨床に採用されるまでには至らなかった．MarinoとMueller-Hermelinkは1985年に腫瘍細胞と胸腺の皮質および髄質における胸腺上皮との類似性を基礎とした組織学的分類を発表していた[6)]．この分類のなかでWell differentiated carcinoma（WDC）と呼ばれるカテゴリーにおいては単一の腫瘍細胞の増生だけでなく，リンパ球の混在があってもよいとし，胸腺に発生する扁平上皮癌などと比較すると予後が良いことが指摘されていた[15)]．WHOは胸腺上皮腫瘍の分類を行うに当たり，各国の病理学者を集めたパネル協議を通じて1999年に基本的にMueller-Hermelinkらの分類に準じた分類を決定して発表した[3)]．それによると，Type Aは核異型のない紡錘形から卵円形の上皮細胞からなり，腫瘍性格を持つリンパ球がほとんどない腫瘍，Type ABはリンパ球に富んだ部位を混じるが基本的には腫瘍細胞がType Aに類似した上皮形態を取る腫瘍，Type B1は正常な機能胸腺の皮質あるいは髄質に存在する胸腺上皮に類似した腫瘍細胞からなる腫瘍，Type B2はリンパ球が多く混在し，空胞化した核とはっきりした核小体を有する腫瘍細胞が散在性認められ，perivascular spaceをよく認めるもの，Type B3は円形から多角形の腫瘍細胞によって占められ，核異型は軽度で，リンパ球の混在の少ないもので，扁平上皮化成やperivascular spaceが通常認められる腫瘍，Type Cは細胞の異型が強く他の臓器の腫瘍で癌と診断すべきもので，リンパ球が混在しても，成熟型のリンパ球や形質細胞であるものとしている．

当科で1985年から2005年までに経験しRetrospectiveにWHO分類による判定を行った胸腺上皮腫瘍131例の予後を解析した．正岡の分類の中には含まれない扁平上皮癌症例を胸腺癌としてあわせて検討した．胸腺癌症例は5年生存で42.9%と不良であった．IVa期症例も5年生存71.1%と早期に再発による死亡が認められた．II期，III期の症例では，予後は良好とはいえ，死亡症例が認められたが，I期症例では良好な予後が得られていた．

WHO分類により予後を検討したところ，Type Cでは5年生存57.1%と不良であった．Type Cの成績は他の群との間に有意差を認めた．他の群の5年生存率はType A 100%，Type AB 100%，Type B1 100%，Type B2 92.6%，Type B3 95.5%とこれらの群間には予後に有意差を認めていない．Okumuraら[7)]，Nakagawaら[16)]の報告では20年以上の観察期間で検討してType B1とType B2，Type B2とType B3の間に有意差を認めている．長期の観察を必要とする胸腺腫の生物学的特徴によるものと考えられる．術後の補助療法の有無が予後に影響を与えている可能性もあると思われる．WHO分類による胸腺腫の予後の検討はMineo[8)]，Rena[17)]らによっても行われ，この分類が腫瘍の悪性度を反映すると報告しているが，いずれの報告でも正岡の病期分類は独立した予後決定因子であることを明らかにしている．

以上の結果から，生存に関しては臨床所見を重視した正岡の分類によるほうが予後を明確に弁別できると考えられた．Wrightらは胸腺腫の再発を予測するのに浸潤の程度，WHO分類と腫瘍径が重要であると報告しており，正岡分類も再発に関与する独立した因子であるとしている[9)]．病理学的分類と臨床所見の立場

からの病期分類を加味して診療に役立てることが重要であると考えられる．

外科治療成績の悪い群では集学的治療を考慮すべきであり，当科では画像診断によって浸潤の有無を判断し，症例を選択して術前化学療法や術後照射を行っている．

当科の症例では，正岡分類のII期の症例では43例中8例に術後照射が行われ，III期症例では23例中18例に術後照射，3例に化学療法が行われ，IVa期症例では15例中10例に術前化学療法を1例に術後化学療法を，照射を12例に行っている．術前に化学療法を行うことで大血管や肺に浸潤する胸腺腫症例において腫瘍の縮小が得られ，合併切除の範囲を縮小することができるため，画像診断で浸潤臓器が明らかな場合には術前化学療法を施行したほうがよいと考えられる．胸腺腫に対する照射の効果については加勢田[18]やUematsuら[19]が少量の全肺照射を含む放射線治療を行うと，照射野内での再発が抑制されるとの報告を行っている．これらの補助療法が本検討の予後を改善している可能性があると考えられる．

また，重症筋無力症合併症例に関しては重症筋無力症の消長と腫瘍の再発の関係が不明であり，術後遠隔期に重症筋無力症のみならず，赤芽球癆や無ガンマグロブリン血症を発症する症例も経験されることなどから今回は検討しなかった．重症筋無力症の合併については予後が不良となるとの報告[20]と，予後に関係しないとの報告[7]がある．最近の多変量解析の結果では予後に影響を与えないと考えられている[7]．

## VI. おわりに

胸腺上皮系腫瘍の外科治療成績は胸腺癌も含め，病理組織学的性格と腫瘍の浸潤傾向によって決定されると考えられた．胸腺上皮系腫瘍の内でも浸潤型胸腺腫および胸腺癌の治療成績は良好とは言えず，この成績を改善するためには集学的治療が不可欠で，生検による病理組織学的検討と画像診断による浸潤傾向の診断を行って術前治療の必要性を判断することが重要であると考えられる．

### 文　献


1) Masaoka A, Monden Y, Nakahara K, et al.: Follou up study of thymoma with special reference to their clinical stages. Cancer, 48 : 2485—2492, 1981.
2) Travis WD, Brambilla E, Muller-Hermelink HK, et al.: World Health Organisation Classification of tumours, International Agency of Research on Cancer (IARC) Pathology and genetics of tumours of the lung, pleura. thymus and heart. IARC Press Lyon, pp145—248, 2004.
3) Rosai J: Histological typing of tumors of the thymus. In: World Health Organization International Histological Classification of the Tumors, 2nd ed, Springer Verlag, New York, Berlin, 1999.
4) Yamakawa Y, Masaoka A, Hashimoto T, et al.: A tentative tumor-node-metastasis classification of thymoma. Cancer, 68 : 1984—1987, 1991.
5) Gamondes JP, Balawi A, Greenland T, et al.: Seventeen years of surgical treatment of thymoma: factors influencing survival. Eur J Cardiothorac Surg, 5 : 124—131, 1991.
6) Marino M, Muller-Hermelink HK: Thymoma and Thymic carcinoma: Relation of thymoma epithelial cells to the cortical and medullary differentiation of the thymus. Virchow Arch A Pathol Anat Histopathol, 407 : 119—149, 1985.
7) Okumura M, Ohta M, Tateyama H, et al.: The World Health Organization histologic classification system reflects the oncologic behavior of thymoma —A clinical study of 273 patients. Cancer, 94 : 624—632, 2002.
8) Mineo TC, Ambrogi V, Mineo D, et al.: Long term disease free survival of patients with radically resected thymomas Relevance of cell-cycle protein expression. Cancer, 104 : 2063—2071, 2005.
9) Wright CD, Wain JC, Wong DR, et al.: Predictors of recurrence in thymic tumors: Importance of invasion, World Health Organization histology, and size. J Thorac Cardiovasc Surg, 130 : 1413—1421, 2005.
10) Rosai J, Levine GD: Tumors of the Thymus. In: Harlan I, Ferminger MD (eds), Atlas of tumor pathology, 2nd series, fascicle 13, The Armed Forces Institute of Pathology, Washington (DC), p144, 1976.
11) Lewis JE, Wick MR, Scheithauer BW, et al.: Thymoma: a clinicopathologic review. Cancer, 60 : 2727—2743, 1987.
12) Gripp S, Hilgers K, Wurm R, et al.: Thymoma; prognostic factors and treatment outcomes. Cancer, 83 : 1495—1503, 1998.
13) Bernatz PE, Harrison EG, Clagett OT: Thymoma: a clinicopathologic study. J Thorac Cardiovasc Surg, 42 : 424—444, 1961.
14) Nomori H, Horinouchi H, Kaseda S, et al.: Evaluation of malignant grade of thymoma by morphometric analysis. Cancer, 61 : 982—988, 1988.
15) Masaoka A, Yamakawa Y, Fujii Y: Well differentiated thymic carcinoma: is it thymic carcinoma or

not? J Thorac Cardiovasc Surg, 117 : 628—630, 1999.
16) Nakagawa K, Asamura H, Matsuno Y, et al.: Thymoma: A clinicopathological study based on the new World Health Organization classification. J Thorac Cardiovasc Surg, 126 : 1134—1140, 2003.
17) Rena O, Papalia E, Maggi G, et al.: World Health Organization histologic classification: An independent prognostic factor in resected thymomas. Ling Cancer, 50 : 59—66, 2005.
18) 加勢田静，堀之内宏久，加藤良一，他：浸潤型胸腺腫に対する少量広範囲照射．胸部外科，46 : 31—34, 1993.
19) Uematsu M, Yoshida H, Kondo M, et al.: Entire hemithorax irradiation following complete resection in patients with stage II-III invasive thymoma. Int J Rad Oncol Biolo Physics, 35 : 357—360, 1996.
20) Maggi G, Casadio C, Cavallo A, et al.: Thymoma: results of 241 operated cases. Ann Thorac Surg, 51 : 152—156, 1991.

## PROGNOSIS OF SURGICALLY TREATED THYMIC EPITHELIAL TUMORS

Hirohisa Horinouchi, Keisuke Asakura, Yoshishige Kimura, Ken Takeuchi, Masafumi Kawamura, Masazumi Watanabe, Keisuke Eguchi and Koichi Kobayashi
Department of Surgery, Keio University School of Medicine, Tokyo, Japan

This study was performed to clarify the prognosis of patients with surgically treated thymic epithelial tumors. The records of 131 patients who underwent surgical treatment during 1985-2005 were retrospectively reviewed. Pathologic review was done according to the WHO classification of tumors of the thymus. Patients characteristics were : 76male and 55fimale ; average age 53 (range 20-80) years ; tumor stage was stage I in 42, stage II in 43, stage III in 23, stage IVa in 15, stage IVb in 1, and thymic carcinoma (squamous cell carcinoma) in 7 based on Masaoka's staging. There were 7 cases of type A, 23 of type AB, 30 of type B1, 27 of type B2, 29 of type B3, and 15 of type C. Surgical procedures performed were 5 partial resections, 5 tumoretomies, 5 thymectomies, 65 extended thymectomies, 4 tumorectomies plus adjunctive resections of surrounding tissue, and 51 extended thymectomies plus tumorectomies plus adjunctive resections of surrounding tissue including the pleura, pericardium, lung, and great vessels. Five-, 10-, and 15-year survival rates by Masaoka stage were 100%, 100%, and 100% in stage I ; 100%, 100%, and 87.5% in stage II ; 100%, 87.5%, and 87.5% in stage III ; 71.1%, 53.3%, and 53.3% in stage IVa ; and 42.9%, 42.9%, and 0% in thymic carcinoma. The prognosis of patients with stage IVa and thymic carcinoma was thus significantly poorer compared with that in the other groups. According to the WHO classification, the 5- year survival rate of type A was 100%, and the 5-, 10-, and 15-year survival rates were 100%, 100%, and 100% in type AB ; 100%, 100%, and 75.0% in type B1 ; 92.6%, 86.4%, and 86.4% in type B2 ; 95.5%, 95.5%, and 81.8% in type B3 ; and 57.1%, 42.9%, and 0% in type C. The survival rate of patients with type C was the poorest and there was a significant difference between type C and all other groups.

The prognosis of patients with thymic epithelial tumors after resection is thought to be determined by histologic classification and clinical invasiveness. In particular, patients with type B3 and type C thymomas should be considered for multidisciplinary treatment.

© Japan Surgical Society　Journal Web Site : http://journal.jssoc.or.jp

World Journal of Surgery

© 2006 by the Société Internationale de Chirurgie
Published Online: 21 July 2006

World J Surg (2006) 30: 1755–1762
DOI: 10.1007/s00268-005-0369-2

# Anti-High-Mobility Group Box Chromosomal Protein 1 Antibodies Improve Survival of Rats with Sepsis

Koichi Suda, MD,[1] Yuko Kitagawa, MD, PhD,[1] Soji Ozawa, MD, PhD,[1] Yoshiro Saikawa, MD, PhD,[1] Masakazu Ueda, MD, PhD,[1] Masahito Ebina, MD, PhD,[2,3] Shingo Yamada, PhD,[4] Satoru Hashimoto, MD, PhD,[5] Shinji Fukata, MD, PhD,[6] Edward Abraham, MD,[7] Ikuro Maruyama, MD, PhD,[8] Masaki Kitajima, MD, PhD,[1] Akitoshi Ishizaka, MD, PhD[9]

[1] *Department of Surgery, School of Medicine, Keio University, Shinanomachi 35, Shinjuku-ku, Tokyo 160-8582, Japan*
[2] *Department of Respiratory Oncology and Molecular Medicine, Department of Thoracic Surgery, Institute of Development, Aging and Cancer, Tohoku University, Sendai, Japan*
[3] *Department of Pathology, Tohoku University School of Medicine, Sendai, Japan*
[4] *Central Institute, Shino-Test Corporation, Kanagawa, Japan*
[5] *Department of Anesthesiology and Intensive Care, Kyoto Prefectural University of Medicine, Kyoto, Japan*
[6] *Department of Surgery, National Center for Geriatrics and Gerontology, Aichi, Japan*
[7] *Division of Pulmonary Sciences and Critical Care Medicine, University of Colorado Health Sciences Center, Denver, CO, USA*
[8] *Department of Laboratory and Molecular Medicine, Kagoshima University, Kagoshima, Japan*
[9] *Department of Internal Medicine, School of Medicine, Keio University, Tokyo, Japan*

**Abstract**

*Background*: High-mobility group box chromosomal protein 1 (HMGB1) has recently been shown to be an important late mediator of endotoxin shock, intraabdominal sepsis, and acute lung injury, and a promising therapeutic target of severe sepsis. We sought to investigate the effect of antibodies to HMGB1 on severe sepsis in a rat cecal ligation and puncture (CLP) model.

*Methods*: Adult male Sprague-Dawley rats underwent CLP and then were randomly divided into two groups: treatment with anti-HMGB1 polyclonal antibodies, and non-immune IgG-treated controls. The serum HMGB1 concentrations were measured at ten time points (preoperatively, and postoperatively at 4, 8, 20, 32, and 48 h and at 3, 4, 5, and 6 days). Hematoxylin-eosin staining, elastica-Masson staining, and immunohistochemical staining for HMGB1 were performed on the cecum and the lung to assess pathological changes 24 h after the CLP procedure.

*Results*: Treatment with anti-HMGB1 antibodies significantly increased survival [55% (anti-HMGB1) vs. 9% (controls); $P < 0.01$]. The serum HMGB1 concentrations at postoperative hours

This work was supported, in part, by Health Sciences Research Grants (Comprehensive Research on Aging and Health 14-015) from the Ministry of Labor Health and Welfare, Japan.

Correspondence to: Yuko Kitagawa, MD, PhD, e-mail: kitagawa@sc.itc.keio.ac.jp

20 and 32 of the anti-HMGB1 antibody-treated animals were significantly lower than those of the controls ($P < 0.05$). Treatment with anti-HMGB1 antibodies markedly diminished the pathological changes and the number of HMGB1-positive cells in the cecum and the lung.
*Conclusions*: The present study demonstrates that anti-HMGB1 antibodies are effective in the treatment of severe sepsis in a rat model, thereby supporting the relevance of HMGB1 eradication therapy for severe sepsis.

High-mobility group box chromosomal protein 1 (HMGB1) is an abundant, highly conserved cellular protein that binds to DNA and stabilizes nucleosome formation, facilitates gene transcription, and regulates the activity of steroid hormone receptors.[1–4] It has recently been shown to be a crucial late mediator of endotoxin shock, fecal peritonitis, and acute lung injury, and is a promising therapeutic target of severe sepsis.[1–4]

Cecal ligation and puncture (CLP) is a commonly used experimental animal model of sepsis.[5–7] This model most closely resembles bowel perforation, with tissue necrosis leading to polymicrobial infection similar to the scenario of acute peritonitis. CLP in rodents results in an early hyperdynamic phase which is followed by a hypodynamic phase, as in human sepsis.[8] Because HMGB1 is actively released into the serum by activated monocyte/macrophages and passively diffuses from necrotic cells, CLP animals have two possible sources of HMGB1: monocyte/macrophages activated by bacterial peritonitis, and necrotic cecum.[9–11]

In 2004, Yang *et al.*[12] reported that—in a murine CLP model—treatment with anti-HMGB1 antibodies and imipenem after CLP surgery significantly increased survival. In the present study, we have modified the conventional CLP model by preserving the feeding artery and the drainage vein. In this model, severe bacterial peritonitis was observed without necrosis of the ligated cecum. We hypothesized that anti-HMGB1 antibodies alone would be effective in modified CLP sepsis and that anti-HMGB1 antibodies would be effective in animals other than mice. The present study was therefore designed to assess whether anti-HMGB1 antibodies alone would have protective effects in a clinically relevant rat sepsis model without necrosis of the cecum.

## MATERIALS AND METHODS

### Animals

Male 8-week-old specific pathogen-free Sprague-Dawley rats, each weighing 250–300 g, were purchased from CLEA Japan (Tokyo, Japan). The animals were allowed to acclimate for 7 days before use in the Laboratory Animals Center, Keio University School of Medicine under standard temperature and light and dark cycles. The rats had access to chow and water ad libitum throughout the study. All procedures were performed with the approval of the Laboratory Animal Care and Use Committee at Keio University School of Medicine.

### Cecal Ligation and Puncture

To establish live intraabdominal infection and sepsis, we subjected the rats to the CLP procedure.[5,6] The animals were first anesthetized by intramuscular injection of ketamine (40 mg/kg of body weight), and a 20-mm midline incision was made to expose the cecum. The cecum was mobilized, ligated below the ileocecal valve while preserving the blood flow of the cecum, then a 5.0-mm blade incision was made at the tip of the cecum. The cecum was replaced in its normal intraabdominal position and the wound closed with a running suture. All animals received saline-solution (0.9% subcutaneously, 5.0 ml/kg of body weight) resuscitation immediately after the surgery.

### Antibody Production

#### Isolation of HMGB1 from porcine thymus chromatin

Porcine HMGB1 was obtained from porcine thymus. HMGB1 was extracted with 0.75 *M* $HClO_4$ and by fractioned precipitation with acetone. Samples were purified by ion-exchange chromatography, (CM-sephadexC25; Pharmacia, Uppsala, Sweden) and analyzed by polyacrylamide gel electrophoresis.

#### Production of anti-HMGB1 polyclonal antibody and control IgG antibody

Porcine HMBG1 was used as immunogen. Hens were injected with porcine HMGB1, and IgG was purified from egg yolk.[13,14] The titration of the antibodies purified was carried out by enzyme-linked immunosorbent assay (ELISA). These anti-HMGB1 polyclonal antibodies were

prepared as previously described.[14] Control IgG antibodies were purified from non-immunized egg yolk.

## Experimental Design

After CLP was performed on Sprague-Dawley rats, they were subcutaneously injected with anti-HMGB1 antibodies (10 mg/kg of body weight) or control antibodies (10 mg/kg of body weight) in a total volume of 500 $\mu$l of sterile saline 15 min after CLP surgery. The dosage of the anti-HMGB1 antibodies was determined based on the least amount that could completely neutralize 3 ng/mL of serum HMGB1 (*i.e.*, the maximal serum HMGB1 concentrations of the control animals) for 24 h *in vitro* (unpublished data). The dosage of the control antibodies was determined to be the same as that of the anti-HMGB1 antibodies. Each group contained 11 animals. Survival was monitored every 4 h for the subsequent 10 days. All of the animals were dissected at death or sacrifice, and intraabdominal and intrathoracic findings were recorded. The surviving animals were killed with diethyl ether on postoperative day (POD) 10.

## Measurements

Blood samples (0.6 mL) were collected from the jugular vein under anesthesia by intramuscular injection of ketamine (40 mg/kg of body weight), centrifuged, and stored at −80°C. The serum HMGB1 concentrations were measured at ten time points [preoperatively, and postoperatively at hours (POH) 4, 8, 20, 32, 48, and at days (POD) 3, 4, 5, and 6 by enzyme-linked immunosorbent assay (ELISA; Central Institute, Shino-Test, Kanagawa, Japan)].[15]

## Histological Evaluations

Cecal ligation and puncture and antibody treatment were performed on two groups of three Sprague-Dawley rats in the same manner as described above. The surviving animals were killed with diethyl ether 24 h after the surgery, and the cecal tissues and the pulmonary tissues were removed from the animals and processed for histologic studies. Hematoxylin-eosin (H&E), elastica-Masson (EM), and immunohistochemical staining for HMGB1 were performed.

## Immunohistochemistry

Formalin-fixed, paraffin-embedded tissues from rat specimens were cut into 4-$\mu$m sections. Each section was mounted on a silane-coated glass slide, deparaffinized, and soaked for 15 min at room temperature in 0.3% $H_2O_2$/methanol to block endogenous peroxidase. Trypsin (Nichirei, Tokyo, Japan) treatment for 10 min at room temperature was performed for antigen retrieval. A murine anti-HMGB1 monoclonal antibody (Central Institute, Shino-Test) was applied for 12 h at 4°C. The primary antibody was visualized using the Histofine Simple Stain MAX-PO(M) kit (Nichirei, Japan) according to the instruction manual.[16] The slide was counterstained with hematoxylin.

## Statistical Analysis

Survival at 10 days was compared by Kaplan-Meier analysis and by log rank statistics, with a $P$ value of less than 0.05 considered to indicate a statistically significant difference. To identify the impact of treatment with anti-HMGB1 antibodies on the time course of changes in serum HMGB1 concentration, we compared the serum HMGB1 concentrations of the animals treated with anti-HMGB1 antibodies (n = 11) and controls (n = 11) at every time point. The comparisons between the data were made with a non-parametric Mann-Whitney $U$-test, with a $P$ value of less than 0.05 considered to indicate a statistically significant difference. To assess the efficacy of treatment with anti-HMGB1 antibodies, an analysis was also performed with the "last observation carried forward" method.[17] The statistical analyses were performed with the StatView 5.0 and SAS statistical analysis package (SAS Institute, Cary, N.C.).

# RESULTS

## Survival Rates

Of the 11 animals treated with anti-HMGB1 antibodies, six survived for 10 days, but only one of the animals treated with control antibodies survived for that same period. A significant difference between the two groups was seen when the whole period of follow up was compared with Kaplan-Meier analysis and log rank test ($P < 0.01$) (Figure 1).

## Time Course of Changes in Serum HMGB-1 Concentrations

Serum HMGB1 concentrations of the controls increased during the first 20 h postoperatively and remained higher than 2 ng/ml thereafter. In contrast, serum HMGB1 concentrations of the animals treated with anti-

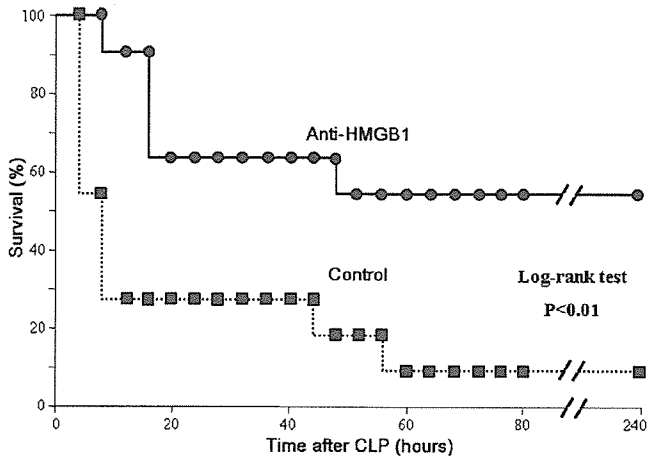


**Figure 1.** Treatment with anti-HMGB1 antibodies improved survival in CLP rats. Survival was analyzed in Sprague-Dawley (SD) rats subjected to CLP, and the treatment with anti-HMGB1 antibodies was started 15 min after CLP surgery. Data are shown as percentages of animals surviving (n = 11 in each group). The whole period of follow up is compared with a Kaplan-Meier analysis and log rank test ($P < 0.01$). ●, anti-HMGB1 antibody-treated group; ■, controls.

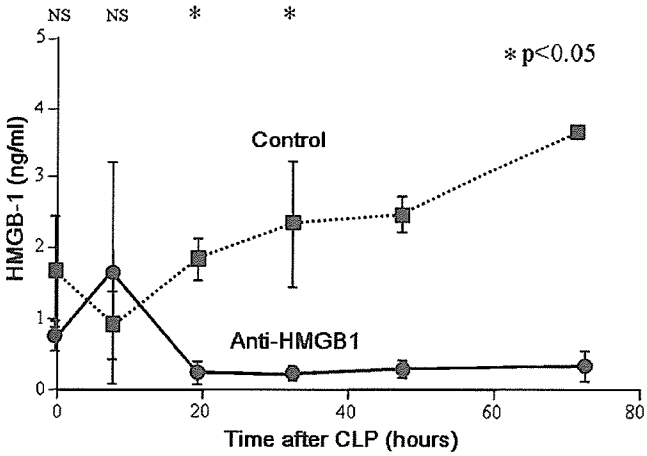


**Figure 2.** Serum HMGB1 concentrations of the animals treated with anti-HMGB1 antibodies were significantly lower than those in the controls at POH 20 and POH 32. Data are shown as means ± SEM of 11 rats in each group. The comparisons between the data at every time point were made with a non-parametric Mann Whitney *U*-test, with *P* values < 0.05 considered to indicate a statistically significant difference. ●, anti-HMGB1 antibody-treated group; ■, controls.

HMGB1 antibodies were significantly lower than in the controls at POH 20 and POH 32, and they remained lower than 0.3 ng/ml (Figure 2).

At POH 4, the serum HMGB1 concentration in the controls had markedly increased ($n = 11$; median: 2.7 ng/ml; interquartile range: 0–11.5 ng/ml), while it had increased to a much lesser extent in the anti-HMGB1

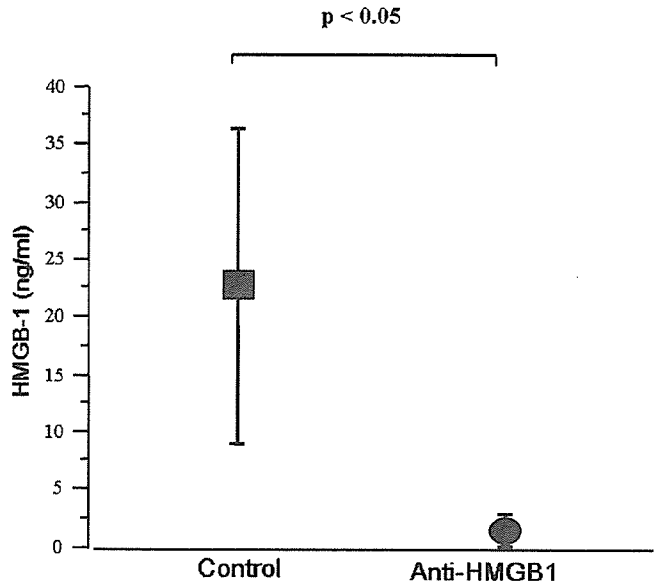


**Figure 3.** To assess the efficacy of treatment with anti-HMGB1 antibodies, we performed an analysis with the "last observation carried forward" method. The levels of the animals treated with anti-HMGB1 antibodies were found to be significantly lower than those of controls ($P < 0.05$ by a non-parametric Mann-Whitney *U*-test).

antibody-treated animals ($n = 11$; median: 0.2 ng/ml; interquartile range: 0–0.55 ng/ml); however, this difference was not statistically significant. Of note, serum HMGB1 concentrations in control animals who died by POH 4 were remarkably high ($n = 5$; median: 18.5 ng/ml; interquartile range: 3.6–82 ng/ml).

The kinetics of serum HMGB1 concentrations tended to correspond with the development of clinical signs of sepsis, such as piloerection, diminished activity, loss of exploratory behavior, and appetite loss. Although most controls developed these signs by POH 8 and succumbed by POD 2, anti-HMGB1 antibody-treated animals were observed to be more alert and active, and only one death occurred after POH 16, as shown in Figure 1.

At the time of death or sacrifice, serum HMGB1 levels in animals treated with anti-HMGB1 antibodies were significantly lower than those of controls ($P < 0.05$ by the "last observation carried forward" method) (Figure 3).

## Intraabdominal and Intrathoracic Findings at the Time of Death or Sacrifice

In both the anti-HMGB1 and control groups, all the animals that died after CLP showed findings typical of diffuse peritonitis, including severe inflammation around the punctured cecum and a large amount of fecal and suppurative ascites. Macroscopic alveolar bleeding and

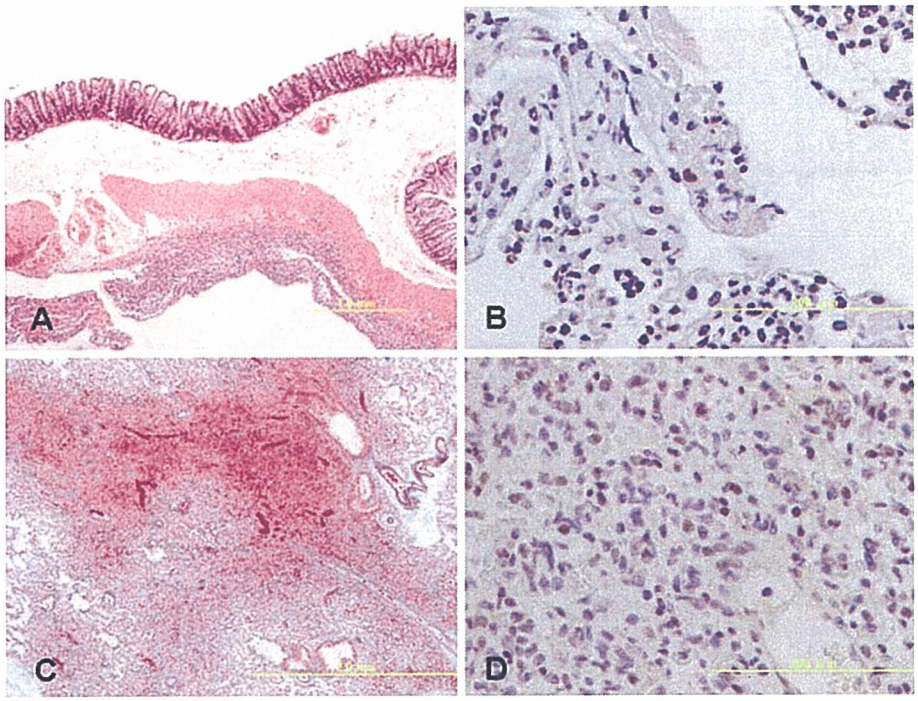


**Figure 4.** Histological and immunohistochemical findings in controls. **A.** H&E staining of the cecum (original magnification, 40×). **B.** Immunohistochemical staining of HMGB1 in the cecum (original magnification, 400×). **C.** Elastica-Masson staining of the lung (original magnification, 40×). **D.** Immunohistochemical staining of HMGB1 in the lung (original magnification, 400×).

pleural effusion were observed in the thoracic cavity of the controls, but such findings were not observed in the anti-HMGB1 antibody-treated animals. In contrast, in both groups, there were no deaths after POD 10. In the surviving animals, the tip of the cecum was covered with intestine and intraabdominal fat tissue, and no foci of acute inflammation or ascites were observed. No remarkable findings were observed in the thoracic cavity or the lungs of the animals who survived POD 10.

The cecums of all the animals both dead and sacrificed were not necrotic but atrophic. No necrosis was observed based on preserving the blood flow of the ileocolic artery and vein according to H&E staining of the cecum of a control at POD 10. No differences were detected between the cecum of the control surviving for 10 days and that of the anti-HMGB1 antibody-treated animals surviving for 10 days.

### Histopathological and Immunohistochemical Findings of the Cecum and the Lung at POH 24

H&E staining of the cecum of the controls showed marked infiltration of inflammatory cells into the subserosa (Figure 4A). The cytoplasm of the erosive mucosa and both nuclei and cytoplasm of many of the inflammatory cells were positively stained for HMGB1 (Figure 4B). Destruction of the pulmonary cell walls, migration of inflammatory cells, and pulmonary hemorrhage were present in the lungs of controls (Figure 4C). In control animals, a large number of HMGB1-positive alveolar macrophage-like cells were present, as were epithelial cells with positive nuclear staining (Figure 4D).

In animals treated with anti-HMGB1 antibodies, H&E staining of the cecum and EM staining of the lung showed almost no destructive or inflammatory changes (Figure 5A, C). Much fewer HMGB1-positive cells were detected in the cecum and the lungs in the anti-HMGB1 antibody-treated group (Figure 5B, D).

## DISCUSSION

Our study yielded two major findings. First, treatment with anti-HMGB1 antibodies after CLP prolonged survival in rats without any antibiotics. Second, serum HMGB1 levels of the controls dramatically increased as early as 4 h after CLP, even though HMGB1 has been considered to be a late mediator of sepsis.

In a previous study, we clarified that the surgical stress of transthoracic esophagectomy itself induced the increase in serum HMGB1, even in patients without complications, and that elevations in HMGB1 might play a contributory role in the development of postoperative organ system dysfunction.[18] Moreover, the patients with sepsis after esophagectomy showed significantly higher serum HMGB1 levels.[18] We proposed that because serum HMGB1 concentrations increased later than inflammatory cytokines, such as IL-1$\beta$, and IL-6, modu-

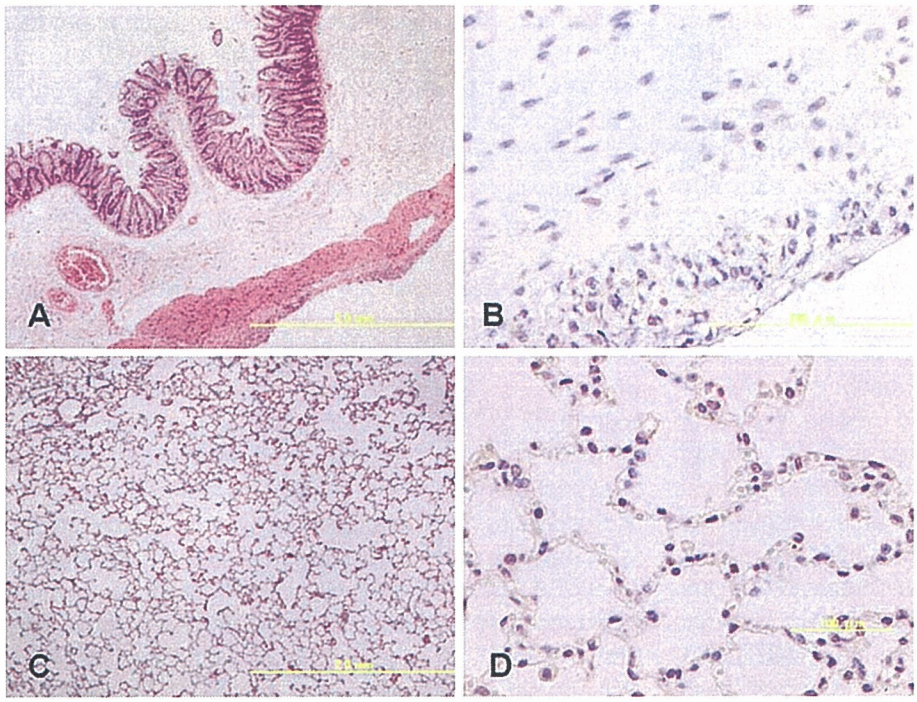


**Figure 5.** Histological and immunohistochemical findings in anti-HMGB1 antibody-treated group. **A.** H&E staining of the cecum (original magnification, 40×). **B.** Immunohistochemical staining of HMGB1 in the cecum (original magnification, 400×). **C.** Elastica-Masson staining of the lung (original magnification, 40×). **D.** Immunohistochemical staining of HMGB1 in the lung (original magnification, 400×).

lating serum HMGB1 concentrations would be more likely to have wider therapeutic windows than modulating serum inflammatory cytokines with the aim of effecting a decrease in surgical stress and an improvement in postoperative clinical courses.[18] With respect to cytokine modulation in esophagectomy, only preoperative administrations of corticosteroid, ulinastatin, and gabexate mesilate have been reported to be effective.[19–21] Working under the consideration that postoperative modulation of serum HMGB1 concentrations might be effective in improving postoperative clinical courses and preventing postoperative complications, we attempted to develop a modified CLP model without antibiotics as a model of systemic inflammatory response syndrom (SIRS)-related multiple organ dysfunction syndrome and to administer anti-HMGB1 antibodies to the model immediately after CLP surgery. In the present study, we developed a modified CLP rat model without necrosis of the cecum by preserving the blood flow of the ileocolic artery and vein. Serum HMGB1 concentrations of the control group rose within 8 h following surgery and were maintained at high concentrations for a period of time, and so we chose subcutaneous injection of anti-HMGB1 antibodies rather than intravenous injection. Because treatment with anti-HMGB1 antibodies alone after CLP significantly prolonged survival in rats without any antibiotics, it is possible to speculate that HMGB1 eradication therapy immediately after surgery may offer a clinically relevant prophylaxis or early intervention to surgical stress-induced organ dysfunction in high-risk cases.

In these experiments, we evaluated the therapeutic effects of anti-HMGB1 antibodies in terms of survival, serum HMGB1 concentrations, and histological changes in the cecum and the lungs. All deaths occurred early, and the marked difference in survival occurred prior to POH 20, actually at POH 12. Serum HMGB1 concentrations of the controls, especially in animals that died, dramatically increased by POH 4, whereas, serum HMGB1 concentrations in anti-HMGB1 antibody-treated animals were significantly suppressed at POH 20 and 32, but this suppression did not begin until POH 8. At POH 24, the inflammatory changes and HMGB1 expression in the cecum and the lungs of the anti-HMGB1 antibody-treated animals were much less than those of the controls. Taken together, these data demonstrate that: (1) anti-HMGB1 antibodies administered subcutaneously 15 min after CLP surgery started to neutralize local and serum HMGB1 between POH 4 and 8 and suppressed both the local inflammatory response as well as inflammation in remote organs, thereby resulting in an improvement in survival; (2) in anti-HMGB1 antibody-treated animals, neutralization of serum HMGB1 as well as suppression of both local and remote inflammation led to suppression of serum HMGB1 concentrations at POH 20 and 32. In the modified CLP model without antibiotics, serum HMGB1 concentrations elevate relatively earlier than in conventional models with sepsis.[1,3,12] Although statistically significant

differences between the anti-HMGB1 antibodies-treated group and the control were not found for serum HMGB1 concentrations at POH 4 because of the large deviation, serum HMGB1 concentrations did increase much earlier and higher in those animals destined to die than in those destined to survive. Moreover, treatment with anti-HMGB1 antibodies significantly prolonged survival. These results suggest that HMGB1 plays a critical role in the induction of the septic physiology around POH 4 and POH 8 in this model.

All animal deaths occurred by POH 56, with none after that, indicating that anti-HMGB1 antibodies did not merely delay death but conferred lasting protection against lethal sepsis.[12] Some control animals survived even without antibiotic treatment. We consider that those controls did well because of the adhesion of the intestines and intraabdominal fat tissue to the perforated cecum. Given that possible scenario, the rats treated with anti-HMGB1 antibodies might have provided time to allow the formation of such adhesions when serum HMGB1 concentrations were maintained below the lethal level, thereby resulting in a greater possibility of recovery from CLP-induced peritonitis.

HMGB1 has recently been recognized as an important late mediator in sepsis.[1–3,12] According to Wang *et al.*[3], in systemic inflammatory responses inflammatory cytokines such as TNF$\alpha$ and IL-1$\beta$ appear in serum transiently, while HMGB1 appears later in the serum as a persistent response. This is the reason why HMGB1 is called a "late mediator". However, the timing of the initial elevation of serum HMGB1 concentrations differs according to the cause of the insults. In murine models of endotoxemia, serum HMGB1 was first detectable 8 h following the administration of an LD50 dose of endotoxin.[1,3] In a murine CLP model, serum HMGB1 levels began to increase significantly 18 h after the induction of peritonitis.[3,12] In murine liver ischemia-reperfusion models, serum HMGB1 concentrations began to elevate as early as 6 h after surgery.[22]

In the present study, serum HMGB1 concentrations of the controls, especially in animals that died, dramatically increased by POH 4, although other early-acting mediators, such as TNF$\alpha$ and IL-1$\beta$, could not be measured because of the limited volume of the blood samples. This result might partially be due to the difference in the cause of the insults and partially to the absence of antibiotic therapy. It is possible that inflammation in CLP rats not treated with antibiotics developed more rapidly than in those treated with antibiotics and, as a result, serum HMGB1 concentrations began to increase at time points earlier than 8 h after CLP surgery. Because macrophages stimulated by endotoxin *in vitro* began to produce HMGB1 4 h after the stimulation, this result did not conflict with the results reported in other studies.[1] Further investigations are required to define the relative phase of the elevation of HMGB1 in comparison with that of other cytokines in the modified CLP model.

We developed the CLP model without necrosis of the cecum by preserving the blood flow of the ileocolic artery and vein. It has been reported that HMGB1 is actively secreted by monocytes and macrophages following stimulation with lipopolysaccharide, TNF-$\alpha$, or IL-1$\beta$, whereas it is passively released from necrotic cells.[1–3,9–11,23–25] HMGB1 secreted actively by the inflammatory cells has also been reported to be structurally different from the HMGB1 released passively by necrotic cells, which is a potent adjuvant.[11] Future studies may be necessary to elucidate possible differences in function between HMGB1 released from monocyte/macrophages and HMGB1 released from necrotic cells. Conventional CLP models develop both bacterial peritonitis and cecal necrosis, but the report of Yang *et al.*[12] on the effect of anti-HMGB1 antibodies in mice subjected to conventional CLP did not distinguish between the source of HMGB1. Consequently, the present study therefore provides novel insights into the function of HMGB1 since these experiments were performed in the absence of any necrosis.

In conclusion, anti-HMGB1 therapy appears to be effective in the treatment of severe sepsis. These results provide impetus to future investigations examining the kinetics of change in serum HMGB1 levels in response to various kinds of insults and also to studies aimed at elucidating the difference between the inflammatory response due to bacterial peritonitis and the inflammatory response due to necrosis.

## ACKNOWLEDGEMENTS

We wish to thank Satoru Fukinbara for advice on statistical analyses. The authors are indebted to Prof. J. Patrick Barron of the International Medical Communications Center of Tokyo Medical University for his review of this manuscript.

## REFERENCES

1. Wang H, Bloom O, Zhang M, *et al.* HMG-1 as a late mediator of endotoxin lethality in mice. Science 1999; 285:248–251.

2. Abraham E, Arcaroli J, Carmody A, *et al.* Cutting edge: HMG-1 as a mediator of acute lung inflammation. J Immunol 2000;165:2950–2954.
3. Wang H, Yang H, Tracey KJ. Extracellular role of HMGB1 in inflammation and sepsis. J Intern Med 2004;255:320–331.
4. Ueno H, Matsuda T, Hashimoto S, *et al.* Contributions of high mobility group box protein in experimental and clinical acute lung injury. Am J Respir Crit Care Med 2004;170:1310–1316.
5. Wichterman KA, Baue AE, Chaudry IH. Sepsis and septic shock—a review of laboratory models and a proposal. J Surg Res 1980;29:189–201.
6. Baker CC, Chaudry IH, Gaines HO, *et al.* Evaluation of factors affecting mortality rate after sepsis in a murine cecal ligation and puncture model. Surgery 1983;94:331–335.
7. Anton EO, Quintela AG, Soto AL, *et al.* Cecal ligation and puncture as a model of sepsis in the rat: influence of the puncture size on mortality, bacteremia, endotoxemia and tumor necrosis factor alpha levels. Eur Surg Res 2001;33:77–79.
8. Heuer JG, Bailey DL, Sharma GR, *et al.* Cecal ligation and puncture with total parenteral nutrition: a clinically relevant model of the metabolic, hormonal, and inflammatory dysfunction associated with critical illness. J Surg Res 2004;121:178–186.
9. Andersson U, Tracey KJ. HMGB1 in sepsis. Scand J Infect Dis 2003;35:577–584.
10. Muller S, Ronfani L, Bianchi ME. Regulated expression and subcellular localization of HMGB1, a chromatin protein with a cytokine function. J Intern Med 2004;255:332–343.
11. Querini PR, Capobianco A, Scaffidi P, *et al.* HMGB1 is an endogenous immune adjuvant released by necrotic cells. EMBO Rep 2004;5:825–830.
12. Yang H, Ochani M, Li J, *et al.* Reversing established sepsis with antagonists of endogenous high-mobility group box 1. Proc Natl Acad Sci USA 2004;101:296–301.
13. Jensenius JC, Andersen I, Hau J, *et al.* Eggs: conveniently packaged antibodies. Methods for purification of yolk IgG. J Immunol Methods 1981;46:63–68.
14. Abeyama K, Stern DM, Ito Y, *et al.* The N-terminal domain of thrombomodulin sequesters high-mobility group-B1 protein, a novel anti-inflammatory mechanism. J Clin Invest 2005;115:1267–1274.
15. Yamada S, Inoue K, Yakabe K, *et al.* High mobility group protein 1 (HMGB1) quantified by ELISA with a monoclonal antibody that does not cross-react with HMGB2. Clin Chem 2003;49:1535–1537.
16. Naito Z, Ishiwata T, Kurban G, *et al.* Expression and accumulation of lumican protein in uterine cervical cancer cells at the periphery of cancer nests. Int J Oncol 2002;20:943–948.
17. Glyn E, Evans V, Sigurgeirsson B. Double blind, randomised study of continuous terbinafine compared with intermittent itraconazole in treatment of toenail onychomycosis. BMJ 1999;318:1031–1035.
18. Suda K, Kitagawa Y, Ozawa S, *et al.* Serum concentrations of high-mobility group box chromosomal protein 1 before and after exposure to the surgical stress of thoracic esophagectomy: a predictor of clinical course after surgery? Dis Esophagus 2006;19:5–9.
19. Ono S, Aosasa S, Mochizuki H. Effects of a protease inhibitor on reduction of surgical stress in esophagectomy. Am J Surg 1999;177:78–82.
20. Sato N, Koeda K, Ikeda K, *et al.* Randomized study of the benefits of preoperative corticosteroid administration on the postoperative morbidity and cytokine response in patients undergoing surgery for esophageal cancer. Ann Surg 2002;236:184–190.
21. Sato N, Endo S, Kimura Y, *et al.* Influence of a Human Protease inhibitor on surgical stress induced immunosuppression. Dig Surg 2002;19:300–305.
22. Watanabe T, Kubota S, Nagaya M, *et al.* The role of HMGB-1 on the development of necrosis during hepatic ischemia and hepatic ischemia/reperfusion injury in mice. J Surg Res 2005;124:59–66.
23. Czura CJ, Yang H, Tracey KJ. High mobility group box-1 as a therapeutic target downstream tumor necrosis factor. J Infect Dis 2003;187:S391–S396.
24. Mitchell BR, Ochani M, Li J, *et al.* IFN-$\gamma$ induces high mobility group box 1 protein release partly through a TNF-dependent mechanism. J Immunol 2003;170:3890–3897.
25. Yang H, Wang H, Tracey KJ. HMG-1 rediscovered as a cytokine. Shock 2001;15:247–253.

# BRCA1 Ubiquitinates RPB8 in Response to DNA Damage

Wenwen Wu,[1] Hiroyuki Nishikawa,[1] Ryosuke Hayami,[1] Ko Sato,[1] Akeri Honda,[1] Satoko Aratani,[2] Toshihiro Nakajima,[2] Mamoru Fukuda,[1] and Tomohiko Ohta[1]

[1]Division of Breast and Endocrine Surgery and [2]Department of Genome Science, Institute of Medical Science, St. Marianna University School of Medicine, Kawasaki, Japan

## Abstract

**The breast and ovarian tumor suppressor BRCA1 catalyzes untraditional polyubiquitin chains that could be a signal for processes other than proteolysis. However, despite intense investigations, the mechanisms regulated by the enzyme activity remain only partially understood. Here, we report that BRCA1-BARD1 mediates polyubiquitination of RPB8, a common subunit of RNA polymerases, in response to DNA damage. A proteomics screen identified RPB8 as a protein modified after epirubicin treatment in BRCA1-dependent manner. RPB8 interacted with BRCA1-BARD1 and was polyubiquitinated by BRCA1-BARD1 *in vivo* and *in vitro*. BRCA1-BARD1 did not destabilize RPB8 *in vivo* but rather caused an increase in the amount of soluble RPB8. Importantly, RPB8 was polyubiquitinated immediately after UV irradiation in a manner sensitive to BRCA1 knockdown by RNA interference. Substitution of five lysine residues of RPB8 with arginine residues abolished its ability to be ubiquitinated while preserving its polymerase activity. HeLa cell lines stably expressing this ubiquitin-resistant form of RPB8 exhibited UV hypersensitivity accompanied by up-regulated caspase activity. Our findings suggest that ubiquitination of a common subunit of RNA polymerases is a mechanism underlying BRCA1-dependent cell survival after DNA damage.** [Cancer Res 2007;67(3):951–8]

## Introduction

Germ line mutation of the cancer susceptibility gene *BRCA1* causes familial breast and ovarian cancer. BRCA1 acts as a hub protein that coordinates many cellular pathways to prevent tumor progression. Accordingly, down-regulation of this key protein by mechanisms other than *BRCA1* gene mutation causes sporadic breast cancer (1). All cells defective in BRCA1 show genomic instability as evidenced by hypersensitivity to DNA damage, the presence of chromosomal abnormalities, and the loss of heterozygosity at multiple loci. These results are likely to stem from the failure of BRCA1 to function in DNA damage repair, transcriptional regulation, apoptosis induction, intra-S or $G_2$-M checkpoint function, and regulation of centrosome duplication (2–4).

Involvement of BRCA1 in multiple cellular processes is logical given its enzymatic function as a ubiquitin ligase (E3). In this capacity, it has the potential to interact with numerous protein substrates and subsequently influence the biological response of a cell at many points. BRCA1 contains an $NH_2$-terminal RING finger domain, a common motif found in ubiquitin ligases. It acquires significant ubiquitin ligase activity when bound to another conformationally similar RING finger protein, BARD1, as a RING heterodimer (5–8). The most common polyubiquitin chain is linked through $Lys^{48}$ of ubiquitin and serves as a signal for rapid degradation of substrates by the proteasome-dependent proteolysis pathway (9). However, BRCA1-BARD1 has the unique capacity to catalyze $Lys^{6}$-linked polyubiquitin chains, and the ubiquitination mediated by BRCA1-BARD1 could signal a process other than degradation (10–13). Deleterious missense mutations in the RING finger domain of BRCA1 found in familial breast cancer abolish the E3 ligase activity of BRCA1-BARD1 (6, 7, 14), indicating that the E3 ligase activity is important for role of BRCA1 as a tumor suppressor.

One of the most significant functional features of BRCA1 is that it is a component of the RNA polymerase II holoenzyme (15, 16). BRCA1 specifically interacts with a large fraction of hyperphosphorylated, processive polymerase II (IIO), in preference to the hypophosphorylated polymerase II (IIA) found at promoters (17). It has been proposed that BRCA1 binds polymerase IIO complexes as part of a genome scanning function for DNA damage (18). However, how BRCA1 affects the polymerase II complexes after DNA damage remains partially understood. In this study, we identify RPB8 (also called hRPB17 or *POLR2H*), a common subunit of all three types of RNA polymerases, as a substrate of BRCA1 E3 ligase and show that BRCA1 ubiquitinates RPB8 immediately after DNA damage. HeLa cell lines stably expressing a ubiquitin-resistant form of RPB8 exhibited UV hypersensitivity, a known phenotype of BRCA1 deficiency. These results indicate a significant role of ubiquitin ligase activity of BRCA1 for cell survival after DNA damage and provide a new aspect of a common subunit of RNA polymerases in DNA damage responses.

## Materials and Methods

**Two-dimensional difference gel electrophoresis.** Methods for fluorescence two-dimensional difference gel electrophoresis (DIGE) and mass spectrometric analysis are reported in the Supplementary Data.

**Plasmids.** cDNA for full-length human RPB8 was amplified by PCR from a MCF10A cell cDNA library using Pfx polymerase (Stratagene, La Jolla, CA). Mammalian expression plasmids for BRCA1, BARD1, ubiquitin, and their mutants were previously described (7, 11). The point mutations to substitute the Lys residue(s) of RPB8 with Arg were produced by site-directed mutagenesis (Stratagene). All plasmids used were verified by DNA sequencing.

**Cell cultures and transfections.** T47D, HCC1937 breast carcinoma cells, HeLa cervical carcinoma cells, and 293T transformed human kidney cells were cultured in DMEM supplemented with 10% FCS and 1% antibiotic-antimycotic agent (Life Technologies, Inc., Grand Island, NY) in 5% $CO_2$ at 37°C. MCF10A normal human breast epithelial cells were grown in DMEM/Ham's F12 (1:1) medium supplemented with 2.5% FCS, 100 ng/mL cholera toxin, 20 ng/mL epidermal growth factor, 500 ng/mL hydrocortisone,

**Note:** Supplementary data for this article are available at Cancer Research Online (http://cancerres.aacrjournals.org/).

**Requests for reprints:** Tomohiko Ohta, Division of Breast and Endocrine Surgery, Department of Surgery, St. Marianna University School of Medicine, Kawasaki 216-8511, Japan. Phone: 81-44-977-8111; Fax: 81-44-976-5964; E-mail: to@marianna-u.ac.jp.

©2007 American Association for Cancer Research.

doi:10.1158/0008-5472.CAN-06-3187

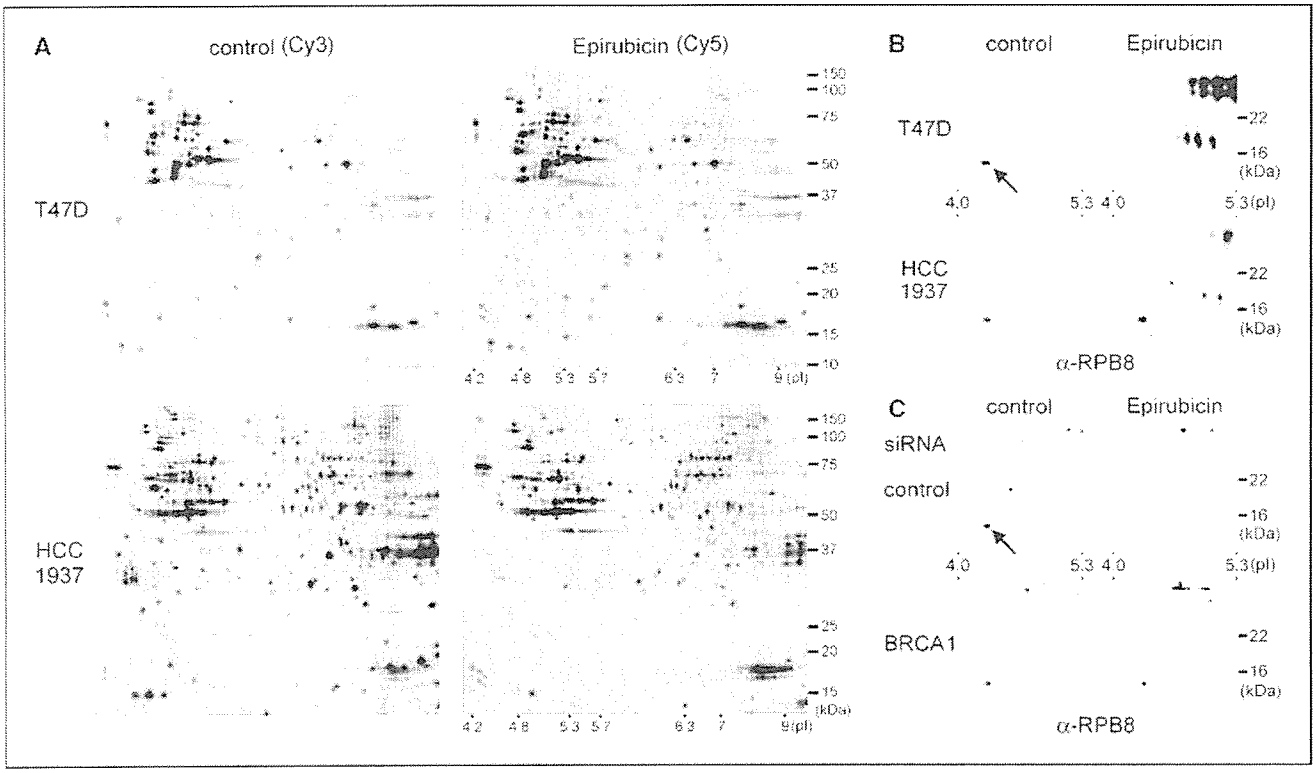


**Figure 1.** Proteomic screen for proteins affected by epirubicin treatment. *A*, T47D cells (*top*) and HCC1937 cells (*bottom*) were either untreated or treated with 0.2 μg/mL of epirubicin for 3 h and lysed with 7 mol/L urea/2 mol/L thiourea–containing buffer. Protein (50 μg) from untreated and epirubicin-treated cells was labeled with Cy3 (*left*) and Cy5 (*right*), respectively. The differently labeled samples were mixed together, resolved on a two-dimensional gel (pH range 3–10, *left* to *right*), and scanned with a fluorescence image analyzer. *Yellow arrows*, protein spots whose levels were significantly altered after epirubicin treatment. *Red arrows*, proteins that significantly decreased only in T47D cells after epirubicin treatment. The slower-migrating protein was identified as RPB8 and the faster one was myosin light chain. *B*, T47D cells or HCC1937 cells were treated as in *A* and lysed with 7 mol/L urea/2 mol/L thiourea–containing buffer. Lysates (500 μg) were resolved on a two-dimensional gel (pH range 3–10). A part of the gel was subjected to immunoblot with anti-RPB antibody. *Arrow*, RPB8. *C*, T47D cells were transfected either with control siRNA (*top*) or with siRNA for BRCA1 (*bottom*), treated with or without epirubicin, and subjected to anti-RPB8 immunoblotting as in *B*.

10 μg/mL insulin, and 1% antibiotic-antimycotic agent. For epirubicin treatment, cells were incubated in medium containing 0.2 μg/mL epirubicin (Pfizer, New York, NY). To examine the half-life of proteins *in vivo*, cells were incubated with 10 μg/mL cycloheximide (Wako, Osaka, Japan), a protein synthesis inhibitor, for the indicated time periods. 293T cells were transfected using the standard calcium phosphate precipitation method. To generate cell lines that stably expressed either wild-type (WT) or mutant FLAG-RPB8, HeLa cells were transfected using FuGENE6 (Roche, Indianapolis, IN) with pcDNA3 plasmids encoding each protein and selected with G418. For UV irradiation studies, cells were washed with PBS, irradiated with UV light (254 nm; UVP, Inc., Upland, CA) at the indicated doses, and grown in fresh medium for various times.

**Antibodies.** Mouse monoclonal antibodies to hemagglutinin (HA; Boehringer-Mannheim, Mannheim, Germany), Myc (BabCo, Richmond, CA), FLAG (Sigma, St. Louis, MO), polyubiquitin (Affiniti, Exeter, United Kingdom), conjugated ubiquitin (Affiniti; ref. 10), α- and β-tubulin (Neomarkers, Fremont, CA), and actin (Santa Cruz Biotechnology, Santa Cruz, CA) as well as rabbit polyclonal antibodies to BRCA1 (Santa Cruz Biotechnology), RPB1 (Covance), and cleaved caspase-3 (Cell Signaling Technology, Danvers, MA) were purchased commercially. Anti-FLAG cross-linked agarose beads (Sigma) were used for immunoprecipitation to detect *in vivo* ubiquitinated substrates. Rabbit polyclonal antibodies to BARD1 and RPC155 were generous gifts from Dr. Richard Baer (Columbia University, New York, NY) and Dr. Nouria Hernandez (Cold Spring Harbor Laboratory, Cold Spring Harbor, NY), respectively. Rabbit polyclonal antibody to RPB8 was generated against full-length human glutathione *S*-transferase (GST)-RPB8 and purified by protein G agarose chromatography.

**RNA interference.** SMART pool BRCA1 small interfering RNA (siRNA) mix and control siRNA mix were purchased from Dharmacon Research, Inc. (Lafayette, CO). RNA duplexes (final concentration 50 nmol/L) were transfected into the cells with Oligofectamine (Invitrogen, Carlsbad, CA) according to the manufacturer's instructions. Retrovirus expressing short hairpin RNA (shRNA) that targets BRCA1 mRNA sequence 5′-CUAGAAAUCUGUUGCUAUG-3′ was created by cotransfecting 293T cells with pGP vector, pE-ampho vector, and pSINsi-hU6 retroviral vector that has previously been subcloned with the oligonucleotide 5′-GATCCGCTAGAAATCTGTTGCTATGTTCAAGAGACATAGCAACAGATTTCTAGCTTTTTTAT-3′ according to the manufacturer's protocol (TaKaRa, Otsu, Japan). Oligonucleotide 5′-GATCCGTAAGGCTATGAAGAGATACTTCAAGAGAGTATCTCTTCATAGCCTTACTTTTTTAT-3′ was used for the retrovirus expressing control shRNA. For infection, HeLa cells were incubated with virus supernatants and fresh culture medium containing 8 μg/mL Polybrene (Sigma). Cells were analyzed 48 h after transfection or infection.

**Immunoprecipitation and immunoblotting.** Immunoprecipitation and immunoblotting methods were previously described (11). For the immunoblotting analysis after two-dimensional gel electrophoresis, cells were lysed with 7 mol/L urea/2 mol/L thiourea–containing buffer as described above. Soluble fractions were prepared with 0.5% NP40-based buffer as previously described (11). Denatured whole-cell lysates were prepared by boiling in Laemmli SDS-loading buffer with 0.1 mol/L DTT.

***In vitro* ubiquitin ligation assay.** Full-length His-FLAG-RPB8 was obtained from BL21/DE3 bacteria cells with isopropyl-L-thio-β-D-galactopyranoside induction by two-step purification using nickel agarose beads followed by anti-FLAG cross-linked agarose beads (Supplementary Fig. S3). Complexes of WT or I26A mutant of FLAG-BRCA1$^{1-772}$ with BARD1 were

purified from transfected 293T cells by anti-FLAG affinity chromatography and FLAG peptide elution. Both WT and I26A mutant complexes contained an ~1:1 ratio of BRCA1 and BARD1 proteins (Supplementary Fig. S3). Rabbit E1 (BIOMOL, Plymouth Meeting, PA) and mammalian ubiquitin (Boston Biochem, Cambridge, MA) were purchased commercially. The *in vitro* reaction was done as previously described (11) with a reaction mixture (30 μL) that contained 0.5 μg His-FLAG-RPB8, 40 ng E1, 0.3 μg UbcH5c, and 0.3 μg each of FLAG-BRCA1$^{1-772}$ and BARD1.

**Runoff transcription assay.** The runoff transcription assay used was described elsewhere (17). Briefly, the runoff template was created by annealing 50 pmol each of a 65-mer oligonucleotide 5′-ATTGGGTAAAGGAGAGTATTTGAGCGGAGGACAGTACTCCGGGTCCCCCCCCCCCCCCCCCCCCC-3′and a complementary 45-mer oligonucleotide 5′-GACCCGGAGTACTGTCCTCCGCTCTTTTACTCTCCTTTACCCAAT-3′ in a 200 μL annealing mixture containing 20 mmol/L Tris (pH 7.4), 1 mmol/L EDTA, and 0.2 mol/L NaCl. Runoff transcription reactions (20 μL) contained 8.25 mmol/L $MgCl_2$, 5 μg of bovine serum albumin, 250 nmol/L nucleotide triphosphates, 5 units of RNase inhibitor, 50 ng of poly(deoxyinosinic-deoxycytidylic acid), 0.05% NP40, 1 pmol of annealed oligonucleotides, and 0.5 μCi of [α-$^{32}$P]CTP. Equilibrated FLAG-RPB8 immunocomplexes bound to M2 beads (10 μL) were added to the reactions (20 μL) and incubated for 40 min at 30°C and stopped with 50 μL of PK buffer (300 mmol/L sodium acetate, 0.2% SDS, 10 mmol/L EDTA, 100 ng tRNA, and 10 μg proteinase K). Reactions were then incubated at 55°C for 20 min, extracted with phenol/chloroform, and precipitated with ethanol. Single-stranded RNA transcripts were resolved under denaturing conditions on 12% polyacrylamide/urea gels and scanned with the Typhoon 9400 image analyzer (Amersham, Piscataway, NJ).

## Results

**Identification of RPB8 as a protein modified in BRCA1-positive cells after epirubicin treatment.** To search for candidate substrates for the BRCA1-BARD1 E3 ligase in response to DNA damage, we used two-dimensional DIGE technology. Breast cancer–derived, BRCA1–positive T47D cells and BRCA1-defective HCC1937 cells were incubated for 3 h with epirubicin, a topoisomerase II inhibitor that induces DNA double strand breaks. Cells were lysed with 7 mol/L urea/2 mol/L thiourea–containing buffer, and the proteomes were compared with untreated cells using two-dimensional DIGE. Interestingly, whereas the expression levels of only a few proteins were affected by the epirubicin treatment in T47D cells, that of ~100 proteins were altered in HCC1937 cells (Fig. 1*A*). Conversely and even more interesting, two proteins whose expression levels were dramatically reduced in T47D cells were not changed in HCC1937 cells (Fig. 1*A*, *red arrows*). Therefore, we speculated that the reduction could depend on the presence of BRCA1. The protein spots were in-gel digested and subjected to nanoscale capillary liquid chromatography-tandem mass spectrometry (LC/MS/MS) analysis. LC/MS/MS analysis revealed that the samples were RPB8, a common subunit of three types of RNA polymerases, and myosin light chain. RPB8 is a very acidic, small protein with a calculated molecular mass of 17.1 kDa and an isoelectric point of 4.34 (19). One of the most significant functional features of BRCA1 is that it is a component of the RNA polymerase II holoenzyme (15, 16). Therefore, we focused on RPB8 for further analyses.

To confirm our mass spectrometry data, we generated a rabbit polyclonal antibody to GST-RPB8 for immunoblot analysis. Cells were treated as in Fig. 1*A*, and immunoblot analysis of the proteins resolved by two-dimensional gels verified that the protein spot was indeed RPB8. It was again severely reduced by epirubicin treatment only in T47D cells (Fig. 1*B*). The difference in RPB8 expression in response to epirubicin treatment could be due to the different genetic backgrounds of these two cell lines, not just the absence or presence of BRCA1. Therefore, we next compared RPB8 expression between isogenic cells with and without knockdown of BRCA1

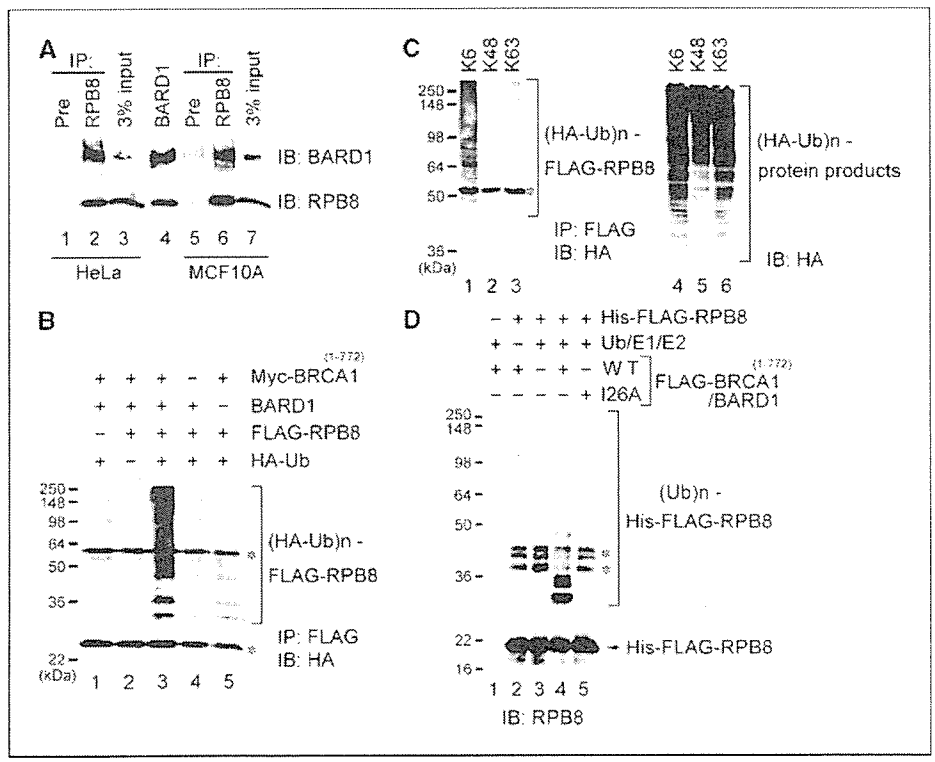


**Figure 2.** RPB8 and BARD1 interaction, and RPB8 ubiquitination by BRCA1-BARD1. *A*, endogenous RPB8 interacts with BARD1. Lysates prepared from HeLa (*lanes 1–3*) or MCF10A (*lanes 5–7*) cells were immunoprecipitated (*IP*) with anti-RPB8 or preimmune serum (*Pre*) and analyzed by immunoblotting (*IB*) using the indicated antibodies. A portion of the cell lysates corresponding to 3% of the input for immunoprecipitation as well as lysate from 293T cells transfected with BARD1 (*lane 4*) were also loaded. *B*, 293T cells transfected with the indicated plasmids were boiled in 1% SDS lysis buffer, diluted to 0.1% SDS, and immunoprecipitated with anti-FLAG antibody–cross-linked beads. Precipitated FLAG-RPB8 was resolved by 12.5% SDS-PAGE followed by immunoblotting with anti-HA antibody. *, IgG. *C*, polyubiquitination of RPB8 was detected as in *A*, except that HA-ubiquitin (*HA-Ub*) with a single lysine residue was transfected as indicated (*lanes 1–3*). A portion of the cell lysate was subjected to immunoblotting with anti-HA antibody to detect total HA-ubiquitin–conjugated proteins in cells as a control for protein expression (*lanes 4–6*). *, IgG. *D*, bacterially purified His-FLAG-RPB8 was incubated in the presence of ATP with ubiquitin, E1, E2/UbcH5c, and either WT or I26A mutant of FLAG-BRCA1$^{1-772}$/BARD1 complex as indicated and immunoblotted with anti-RPB8 antibody. *, nonspecific products copurified with His-FLAG-RPB8.

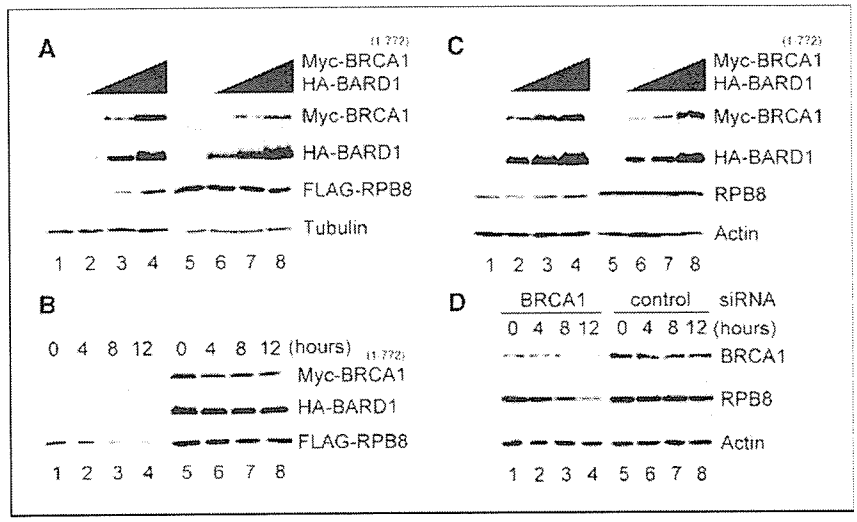


**Figure 3.** BRCA1-BARD1 did not destabilize RPB8 *in vivo* but rather caused an increase of RPB8 in the soluble fraction. *A*, 293T cells were transfected with plasmids encoding FLAG-RPB8 (*lanes 1–8*, 0.3 μg) and increasing amounts of Myc-BRCA1$^{1-772}$ and HA-BARD1 (*lanes 2* and *6*, 2 μg; *lanes 3* and *7*, 4 μg; *lanes 4* and *8*, 7.35 μg each). Total plasmid DNA was adjusted to 15 μg per plate by adding the parental pcDNA3 vector. The steady-state level of each protein in the soluble fraction (*lanes 1–4*) and whole-cell lysates (*lanes 5–8*) was analyzed by immunoblot using anti-Myc, anti-HA, anti-FLAG, or anti-tubulin antibodies. *B*, 293T cells were transfected with plasmids encoding FLAG-RPB8 (0.2 μg) and either parental pcDNA3 vector (2 μg, *lanes 1–4*) or Myc-BRCA1$^{1-772}$ and HA-BARD1 (1 μg each, *lanes 5–8*). Thirty-six hours after transfection, cells were incubated with cycloheximide (10 μmol/L) and chased for the indicated lengths of time. Soluble fractions of the cell lysates were then immunoblotted with Myc, HA, or FLAG antibody. *C*, steady-state levels of RPB8 were analyzed as in *A*, except that FLAG-RPB8 was not transfected and anti-RPB8 antibody was used to detect endogenous RPB8. *D*, T47D cells were transfected either with siRNA for BRCA1 (*lanes 1–4*) or control siRNA (*lanes 5–8*). Cells were incubated with cycloheximide (10 μmol/L) and chased for the indicated lengths of time. The soluble fraction of the cell lysates was then immunoblotted with the indicated antibodies.

expression. T47D cells were transfected with either control siRNA or BRCA1 siRNA and then treated as in Fig. 1*A*. The siRNA-transfected cells were successfully silenced for BRCA1 expression (Supplementary Fig. S1). Immunoblot analysis of the proteins resolved by two-dimensional gels showed that RPB8 was reduced by epirubicin treatment only in control cells, not in cells with BRCA1 knockdown, supporting the idea that this modification depends on BRCA1 expression (Fig. 1*C*). The reduction of RPB8 at its normal migrating position could be due to protein degradation or to covalent modification.

**BRCA1-BARD1 interacts with and ubiquitinates RPB8.** The polymerase II holoenzyme interacts with BRCA1 and BARD1 (15, 16). Consistent with the previous reports, a significant amount of endogenous BARD1 coimmunoprecipitated with RPB8 isolated from HeLa cells or MCF10A cells compared with controls (Fig. 2*A*). The same results were observed with MCF7, T47D, and 293T cells (data not shown). Exogenously expressed RPB8 also interacted with BRCA1 and BARD1 (Supplementary Fig. S2). Then, we tested whether RPB8 is ubiquitinated by BRCA1-BARD1 *in vivo*. FLAG-RPB8 was coexpressed in 293T cells with HA-ubiquitin, Myc-BRCA1$^{1-772}$, and BARD1. Cells were collected 36 h after transfection and boiled in 1% SDS–containing buffer, and FLAG-RPB8 was immunoprecipitated. Immunoblotting of the RPB8 precipitates resolved by SDS-PAGE using anti-HA antibody showed a ladder characteristic of polyubiquitinated RPB8 (Fig. 2*B*). Omission of FLAG-RPB8, HA-ubiquitin, Myc-BRCA1$^{1-772}$, or BARD1 all abolished the RPB8 ladders, supporting the idea of BRCA1-BARD1–dependent RPB8 ubiquitination.

BRCA1-BARD1 is the only known E3 ligase to catalyze Lys$^6$-linked polyubiquitin chains (10, 11, 13). To show that the *in vivo* RPB8 ubiquitin ladders were directly due to BRCA1-BARD1 ligase activity, we verified that RPB8 was modified by ubiquitin through Lys$^6$ linkages. HA-tagged ubiquitins that have a single lysine residue available for conjugation were used for *in vivo* ubiquitination assays. As expected, BRCA1-BARD1–dependent RPB8 polyubiquitination was predominantly detected when HA-ubiquitin with only Lys$^6$ available, but not Lys$^{48}$ or Lys$^{63}$, was coexpressed (Fig. 2*C*). However, it has been suggested that ubiquitin mutants could fold incorrectly and may cause artifacts (20). Recent quantitative analysis of *in vitro* ubiquitination revealed that even for cyclin B1 ubiquitination catalyzed by the anaphase-promoting complex, heterogeneous ubiquitin chains, including Lys$^{63}$, Lys$^{11}$, and Lys$^{48}$, or monoubiquitin attached to multiple lysine residues on the substrate. Further, some types of linkages are dependent on the combination of E2 and E3 enzymes (21). Thus, it is possible that ubiquitination mediated by BRCA1-BARD1 also resulted in multiple polyubiquitin chains, including Lys$^6$. The preference for Lys$^6$ ubiquitination observed in the *in vivo* experiment was not enough evidence to support the direct role of BRCA1-BARD1 for RPB8 ubiquitination. Therefore, we further tested whether BRCA1-BARD1 directly catalyzes RPB8 polyubiquitination by *in vitro* ubiquitination using recombinant RPB8 protein (Supplementary Fig. S3). His-FLAG-RPB8 incubated with ubiquitin, E1, E2/His-UbcH5c, and FLAG-BRCA1$^{1-772}$/BARD1 complex (Supplementary Fig. S3) resulted in a ladder and smear detected by anti-RPB8 immunoblot (Fig. 2*D*). Omission of substrate RPB8, ubiquitin/E1/E2, or FLAG-BRCA1$^{1-772}$/BARD1 complex, as well as substitution of BRCA1$^{1-772}$ with the E2-nonbinding mutant I26A, all abolished RPB8 ubiquitination. Hence, the results suggest that the RPB8 polyubiquitination is directly catalyzed by BRCA1-BARD1.

**BRCA1-BARD1 does not destabilize RPB8 *in vivo*.** Our previous results suggested that BRCA1-BARD1 catalyzed untraditional polyubiquitin chains that served as a signal for a process other than degradation (7, 11, 12). However, the reduced expression of RPB8 after epirubicin treatment detected by two-dimensional DIGE or two-dimensional immunoblot (Fig. 1) suggested the

possibility of BRCA1-mediated RPB8 degradation. Therefore, we tested if BRCA1-BARD1 destabilized RPB8 *in vivo* under several different conditions, including BRCA1-BARD1 overexpression and BRCA1 knockdown by siRNA. FLAG-RPB8 was coexpressed in 293T cells with Myc-BRCA1$^{1-772}$ and HA-BARD1 (Fig. 3*A*). The steady-state level of FLAG-RPB8 increased upon coexpression of BRCA1-BARD1 in a dose-dependent manner in the soluble fraction (*lanes 1–4*) but not in whole-cell lysates (*lanes 5–8*). We then examined protein half-life of FLAG-RPB8 in the soluble fraction using cycloheximide, a protein synthesis inhibitor. The FLAG-RPB8 protein half-life was prolonged by BRCA1-BARD1 overexpression (Fig. 3*B*). We also tested the effect of BRCA1-BARD1 on endogenous RPB8 (Fig. 3*C* and *D*). The steady-state level of RPB8 only slightly increased upon coexpression of BRCA1-BARD1 in the soluble fraction (Fig. 3*C*, *lane 4*) and no effect was observed when whole-cell lysates were evaluated (*lanes 5–8*). However, RPB8 protein half-life was detectably shortened by BRCA1 knockdown (Fig. 3*D*). This observation was not detected when whole-cell lysates were analyzed (data not shown). Together, analyses of steady-state levels and protein half-lives indicated that only soluble RPB8 was stabilized, whereas that in whole-cell lysate was unchanged (Fig. 3). Alternatively, it was also possible that BRCA1-BARD1 shifted RPB8 from the insoluble fraction, such as the chromatin fraction, to the soluble fraction. However, we could not detect such a shift by fractionation analyses (data not shown). In either case, these findings at least suggest that BRCA1-BARD1–mediated RPB8 ubiquitination is not a signal for its degradation.

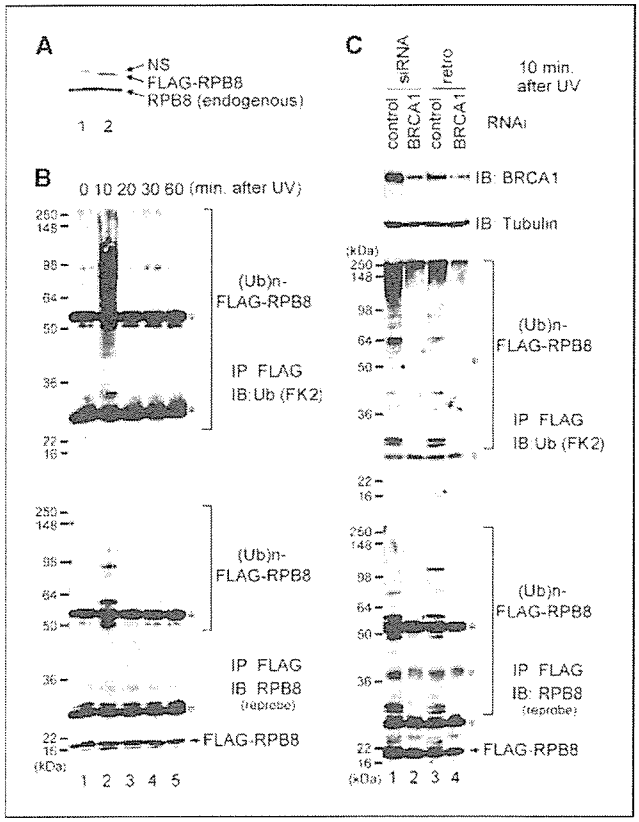


**Figure 4.** BRCA1-dependent RPB8 polyubiquitination in response to UV irradiation. *A*, parental HeLa cells (*lane 1*) and HeLa cells stably expressing FLAG-RPB8 (*lane 2*) were lysed with SDS-sample buffer and immunoblotted with anti-RPB8 antibody. *NS*, nonspecific products. *B*, HeLa cells stably expressing FLAG-RPB8 were UV irradiated (35 J/m$^2$) and harvested at the indicated times after irradiation. Ubiquitinated RPB8 was detected as described in Fig. 2*B*, except that anti-ubiquitin antibody (FK2) was used for immunoblotting (*top*). The membrane was reprobed with anti-RPB8 antibody (*bottom*). *C*, HeLa cells stably expressing FLAG-RPB8 were either transfected with control siRNA (*lane 1*), transfected with siRNA for BRCA1 (*lane 2*), infected with retrovirus expressing control shRNA (*lane 3*), or infected with retrovirus expressing shRNA for BRCA1 (*lane 4*). Cells were then UV irradiated (35 J/m$^2$) and harvested 10 min after irradiation. Cells were boiled in 1% SDS buffer and subjected either to immunoblotting with anti-BRCA1 (*top*) and antitubulin (*upper middle*) or to detection of RPB8 ubiquitination as in *B* (*lower middle* and *bottom*). *, IgG. Note that the different pattern of IgG detection between *B* and *C* is due to different lots of anti-FLAG cross-linked agarose beads.

**BRCA1-dependent RPB8 ubiquitination after UV irradiation.** BRCA1-mediated RPB8 ubiquitination prompted us to investigate the biological implications of this activity. We examined if RPB8 is ubiquitinated in response to DNA damage. Rather than exposing cells continuously to epirubicin, and because RPB1 is ubiquitinated after UV irradiation, we used UV irradiation to accurately determine the timing of RPB8 ubiquitination after DNA damage (22–25). We established HeLa cell lines that stably express FLAG-RPB8 at a low level (approximately one third of endogenous RPB8; Fig. 4*A*) to avoid artifacts caused by overexpression and analyzed ubiquitination of anti-FLAG immunoprecipitates with anti-ubiquitin (FK2) antibody. Because it has been reported that RPB1 ubiquitination occurs 1 to 2 h after UV irradiation (22–25), we first analyzed these time points. However, we did not detect any ubiquitination of FLAG-RPB8 (Fig. 4*B* and data not shown). Instead, ubiquitinated FLAG-RPB8 readily, and only transiently, appeared 10 min after UV irradiation (Fig. 4*B*, *top*). Reprobing the membrane with anti-RPB8 antibody verified that the detected ladder was ubiquitinated RPB8 (*bottom*).

To verify that UV irradiation–induced RPB8 ubiquitination requires endogenous BRCA1, RNA interference was used to knock down BRCA1 expression. HeLa cells stably expressing FLAG-RPB8 were transfected with BRCA1-specific siRNA. As a second alternative, we constructed a retrovirus engineered to express shRNA for BRCA1. Forty-eight hours after transfection or infection, cells were irradiated with UV (35 J/m$^2$) and then harvested 10 min later. Both the siRNA-transfected and the shRNA retrovirus–infected cells were successfully silenced for BRCA1 expression (>90% and >75% reduction, respectively) compared with their controls (Fig. 4*C*, *top*). As expected, RPB8 ubiquitination after UV irradiation was dramatically reduced by BRCA1 knockdown in both cases (*lower middle*). Reprobing the membrane with anti-RPB8 antibody again verified the ubiquitinated RPB8 that became completely undetectable upon BRCA1 knockdown (*bottom*). These results support the idea that RPB8 is polyubiquitinated by BRCA1-BARD1 in an early phase after UV irradiation.

**A ubiquitin-resistant form of RPB8 retains its polymerase activity.** For the purpose of studying the physiologic consequences induced by the BRCA1-mediated RPB8 ubiquitination after UV irradiation, we generated a mutant of RPB8 that is incapable of being ubiquitinated by BRCA1-BARD1. RPB8 possesses eight Lys residues in the whole protein (Fig. 5*A*). We first mutated single Lys residues of RPB8 and tested its capacity to be ubiquitinated. However, RPB8 ubiquitination was not dramatically reduced by each single mutation (Fig. 5*B*, *lanes 2* and *7*; data not shown). Instead, the ubiquitination of RPB8 was reduced as the number of Lys to Arg substitutions increased. This result recapitulates what we observed during studies of BRCA1 auto-ubiquitination and of BRCA1-mediated NPM1/B23 ubiquitination. When five of the eight Lys residues were substituted with Arg (5KR), RPB8 ubiquitination